Journal of Solid Mechanics Vol. 10, No. 2 (2018) pp. 300-314

Determination of Optimal Parameters for Finite Plates with a Quasi-Square Hole

M. Jafari *, M. H. Bayati Chaleshtari , E. Ardalani

Department of Mechanical Engineering, Shahrood University of Technology, Shahrood, Iran

Received 16 February 2018; accepted 7 April 2018

ABSTRACT

This paper aims at optimizing the parameters involved in stress analysis of perforated plates, in order to achieve the least amount of stress around the square-shaped holes located in a finite isotropic plate using metaheuristic optimization algorithms. Metaheuristics may be classified into three main classes: evolutionary, physics-based, and swarm intelligence algorithms. This research uses Genetic Algorithm (GA) from evolutionary algorithm category, Gravitational Search Algorithm (GSA) from physics-based algorithm category and Bat Algorithm (BA) from Swarm Intelligence (SI) algorithm category. The results obtained from the present study necessitate the determination of the actual boundary between finite and infinite plate for the plates with square-shaped holes. The design variables such as bluntness, hole orientation, and plate dimension ratio as effective parameters on stress distribution are investigated. The results obtained from comparing BA, GA and GSA indicate that BA as SI algorithm category competitive results, proper convergence to global optimal solution and more optimal stress level than the two mentioned algorithms. The obtained results showed that the aforementioned parameters have a significant impact on stress distribution around a square-shaped holes and that the structure's load-bearing capability can be increased by proper selection of these parameters without needing any change in material properties.

Keywords: Isotropic finite plate; Analytical solution; Complex variable method; Metaheuristic algorithms.

1 INTRODUCTION

THE determination of optimum shape of holes with minimum stress concentration in finite isotropic plates under uniaxial loading is an important engineering problem. These holes are mostly created in plates to cut the weight of structure or to create points of entry and exit. These holes change the plate geometry and lead to severe local stresses called stress concentration around the holes. Stress concentration reduces strength and cause premature failures in the structures and plastic deformations at the point of stress concentration. Experience has shown that most failures created in aerial structures originate from the presence of stress concentration in structural fittings and fasteners. Knowing the stress concentration factor (SCF) is crucial in achieving optimal design. Therefore, in the design of structures to achieve convenient and efficient design, the study of the effects of geometrical defects in structures is very important.

* Corresponding author. Tel.: +98 9153213144.
E-mail address: m_jafari821@shahroodut.ac.ir (M. Jafari).

2 LITERATURE REVIEW

Much research has been conducted on the stress analysis of isotropic plates with numerical, experimental and analytical approaches. Muskhelishvili [1] used complex variables method to solve the boundary value problems in two-dimensional elasticity. Materials applied in this study were assumed homogeneous, isotropic and linearly elastic. By using the complex variables method and conformal mapping, Savin [2] solved the infinite plate with a rounded triangular hole. The anisotropic plates containing circular and elliptical holes were analyzed by Lekhnitskii [3]. Theocaris et al. [4] studied the stress distribution around equilateral triangular hole also investigated the effect of the curvature of hole corner. Using the complex potential method, the stress distribution around triangular hole in an anisotropic plate was presented by Daoust et al. [5]. In their research bluntness as important parameter in stress analysis of isotropic plates was studied. Abuelfoutouh [6] formulated the circumferential stress around different holes such as elliptical, circular, triangular and square holes in composite shells by defining a special conformal mapping. In addition, Rezaeepazhand and Jafari [7] presented the analytical solution to study the anisotropic plates with holes. They also obtained stress concentration factor for different shapes of hole in metallic infinite plates and pursued the effect of the bluntness and loading directions on the stress concentration [8]. Odishelidze et al. [9] studied stress concentration factor in an elastic square plate with a full-strength hole. He used Kolosov–Muskhelishvili formulas for investigating and the solution was written in quadrature forms. Sharma [10] presented the stress distribution around circular, elliptical and triangular holes for orthotropic laminates and anisotropic plates by means of Muskhelishvili's solution. Kradinov et al. [11] showed application of genetic algorithm in optimal design of bolted composite lap joints. In this research, the laminate thickness, laminate lay-up, bolt location, bolt flexibility, and bolt size were considered as design variables for maximizing the strength of the joint. Yun [12] concerned with high stress concentrations in stiff-fiber reinforced composites, which causes low strengths of materials. Fuschi et al. [13] studied plane stress problems in nonlocal elasticity. He discussed an enhanced computational version of the finite element method in the context of nonlocal strain-integral elasticity of Eringen-type. Rezaeepazhand et al. [14] investigated torsional analysis of hollow bars with specially shaped non-circular cross-sections. He used to complex variable theory for solve the torsion problem and obtain an expression for shear stresses, angle of twist and cross-sectional warping. Ghugal and Sayyad [15] applying shear deformation method to solve the isotropic plates problems. Pan et al. [16] presented the modified stress functions for solving the stress distribution problem of a finite plate with a rectangular hole subjected to uniaxial tension. They used the mapping function presented by Sharma based on Schwarz–Christoffel and studied finite isotropic plate containing rectangular hole. The rectangular hole and the finite area external to the rectangular hole in z-plane were mapped respectively into a unit circle and the finite area outside a unit circle in ζ-plane by using mapping function. Based on Muskhelishvili's complex variable method, two modified stress functions which are and in ζ-plane were proposed. The unknown coefficients of the modified stress functions were determined by enforcing the stress functions to satisfy the stress boundary conditions around the unit circle in ζ-plane and the stress boundary conditions along external boundary in z-plane. Then, the stress field of a finite plate with a rectangular hole was calculated. Jafari and Ardalani [17] studied stress distribution around the different holes in a finite metallic plate, using the complex variable method and the expansion of research conducted by Pan et al. By using the finite element method, Liu and et al. [18] investigated the optimization of the composite plates with multiple holes. At first, they considered the effect of the number of holes and hole spacing relative to each other. The Tsai-Hill failure criterion for a composite plate was used to evaluate cost function. Sivakumara et al. [19] studied the optimization of laminate composites containing an elliptical hole by genetic algorithm method. In this research design variables were the stacking sequence of laminates, thickness of each layer, the relative size of hole, hole orientation and ellipse diameters. The first and second natural frequencies were considered as cost function. Almeida and Awruch [20] studied the optimal design of laminate composites using the genetic algorithm and the finite element approaches. Fiber angle and thickness of each layer were considered as design variables and the cost function was to achieve the lowest deflection and weight. Based on the particle swarm optimization and the finite element method, Chen et al. [21] presented an optimization method for designing reliability of composite structures. In this method, data are exchanged between the ANSYS and MATLAB software. They presented numerical examples for laminates, composite cylindrical shells and composite pressure vessel to prove the effectiveness of his method. Lopez et al. [22] studied an approach for the reliability based design optimization of laminated composites with Particle Swarm Optimization (PSO) method. Vosoughi and Gerist [23] presented a new mixed method of particle swarm optimization, finite element and continuous genetic algorithm to determine the damage of composite beams. At first, they obtained the equilibrium equations governing the composite beam using the first-order shear deformation theory (FSDT) and then by using the finite element method, they solved the resulting equations with related

boundary conditions. After that, they presented their method to check the damage detection. To prove the efficiency of their approach, they dealt with the effect of different parameters such as the loss ratio, the number of damage elements, the fiber angle of each layer and the number of layers on damage assessment of composite beam. Sharma et al.[24] conducted the optimal design of the symmetrical laminates containing an elliptical hole by using the genetic algorithm method. They obtained optimum fiber angle in symmetrical laminated composites with an elliptical hole under in-plane loading conditions. Cost function was calculated by using the Tsai-Hill failure criterion. Design variables were stacking sequence of laminates. Jafari and Rohani [25] studied the optimization of perforated composite plates under tensile stress using genetic algorithm method. The analytical solution was used to determine the stress distribution around different holes in perforated composite plates. Moreover, Suresh et al.[26] investigated the particle swarm optimization approach for multi-objective composite box-beam design. Vigdergauz [27] proposed minimum stress variation as a profound generalization of the equi-stress principle in the shape optimization problem for regular perforated structures in 2D elasticity. Due to its integral nature the new criterion was easily incorporated in the standard GA searching tool which employed complex variables and conformal mapping technique for the cost function of any admissible hole shape. Zhu and et al. [28] considered the optimization of composite strut using the genetic algorithm method and Tsai-Hill failure criterion. Their attention was paid to minimize the weight of structure and increase buckling load. Fiber volume fraction and stacking sequence of laminates were considered as design variables. Campbell et al. [29] investigated injecting problem-dependent knowledge to improve evolutionary optimization search ability. Yang et al. [30] proposed an optimization procedure combining an automated finite element modelling technique with a ground structure approach for structural layout and sizing design of aircraft wings. Rasoli et al. [31] investigated the optimum parameters for determination of stress and strain curves. They used optimization technique and finite element method for solve the problem.

In this study by using the three different categories of optimization algorithms, the optimal values of parameters such as bluntness, rotation angle of hole, and plate dimension ratio that lead to lowest possible stress level around the square-shaped hole in a finite perforated plate under uniaxial loading were calculated. It is worth mentioning that the stress concentration factor value around the hole is considered as cost function (C.F.) for three optimization algorithm. The main goal of this paper is to obtain the optimal design variables which minimize the maximum stress around quasi-square hole calculated by analytical method based on complex variable method.

3 THEORY ANALYSIS

A plate with a hole in the center is available. The ratio of hole side to the longest side of the plate is greater than 0.2. Then, the plate can be considered as finite. The problem is evaluated based on the assumption of presence of in-plane stress and absence of volumetric forces. Hole can rotate relative to the x-axis. Stress-strain relationship is linear. According to Fig. 1, the hole is located in the center of the plate, and because of the traction-free boundary conditions on the edge of the hole, the only stress induced around the hole is σ_θ ($\sigma_\rho = \sigma_{\rho\theta} = 0$).

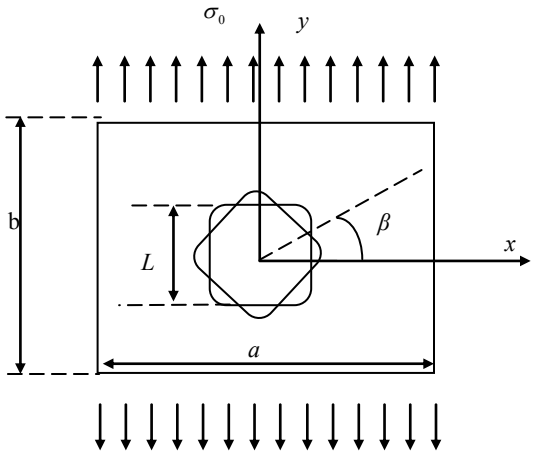

Fig.1
The finite plate with square hole subjected to uniaxial loadings.

This study applied an appropriate mapping function and Muskhelishvili's complex variable method investigating the stress distribution around the hole with different shapes in finite perforated plates. Compatibility equation for perforated materials in plane stress state in terms of stress function U is as follows:

$$\frac{\partial^4 U}{\partial x^4}+2\frac{\partial^4 U}{\partial x^2 \partial y^2}+\frac{\partial^4 U}{\partial y^4}=0 \tag{1}$$

Muskhelishvili showed that the solution of the Eq. (1) can be written as follows:

$$U(x,y)=\mathrm{Re}[\bar{z}\varphi(z)+\theta(z)] \tag{2}$$

After finding U(x,y) in terms of the functions $\varphi(z)$ and $\psi(z)=\theta'(z)$ the stress components in two-dimensional and simply-connected region is calculated as follows [1]:

$$\sigma_x+\sigma_y=4\,\mathrm{Re}\left[\varphi'(z)\right] \tag{3}$$

$$\sigma_y-\sigma_x+2i\,\tau_{xy}=2(\bar{z}\varphi''(z)+\psi'(z)) \tag{4}$$

where $\psi(z)$ and $\varphi(z)$ are the holomorphic functions in terms of the complex variable z. By using a general conformal mapping function as Eq. (5), the hole with different shapes in z-plane is mapped into a unit circle while the corresponding finite area external to the polygonal hole in z-plane is mapped into a finite area outside the unit circle in ζ-plane. In Eq. (5), since R, which is a positive and real number, affects only the size of the hole and not the shape of the curve, its value has no effect on stress distribution around the hole, hence it can be assumed that R=1. Integer n in the mapping function represents the shape of the hole. The hole sides are given by n+1. Parameter m determines the bluntness factor and changes the radius of curvature at the corner of the hole. As shown in Fig. 2, different bluntness can be developed in hole corners with varying m. It should be noted that m=0 is equivalent to a circular hole. In this article, n equal 3 an m between [0, 0.2] and the ratio L/a equals to 0. 4.

m=0 m=0.05 m=0.1 m=0.15 m=0.2

Fig.2
The effect of parameter m on the hole shape.

Using Eq. (6), the x and y coordinate values of the points on hole boundary in z-plane in terms of the θ and ρ coordinate values in ζ-plane are in the form of the Eqs. (7) and (8). In the following equations *Re* and *Im* are real and imaginary parts of the terms in brackets.

$$z=x+iy=\omega(\zeta)=R\left(\zeta+\frac{m}{\zeta^n}\right) \tag{5}$$

$$\zeta=\rho e^{i\theta}=\rho(\cos\theta+i\,\sin\theta) \tag{6}$$

$$x=\mathrm{Re}\left[\omega(\zeta)\right]=R\left(\rho\cos(\theta)+\frac{m\cos(n\theta)}{\rho^n}\right) \tag{7}$$

$$y=\mathrm{Im}\left[\omega(\zeta)\right]=R\left(\rho\sin(\theta)+\frac{m\sin(n\theta)}{\rho^n}\right) \tag{8}$$

The stress components in the curvilinear coordinates (ρ,θ) expressed by the mapping function are:

$$\sigma_\rho+\sigma_\theta=\sigma_x+\sigma_y=4\,\mathrm{Re}\left[\frac{\varphi'(\zeta)}{\omega'(\zeta)}\right] \tag{9}$$

$$\sigma_\theta-\sigma_\rho+2i\,\tau_{\rho\theta}=(\sigma_y-\sigma_x+2i\,\tau_{xy})e^{2i\alpha}=\frac{2\zeta^2}{\rho^2\overline{\omega'(\zeta)}}(\overline{\omega(\zeta)}\varphi'(\zeta)+\omega'(\zeta)\psi(\zeta)) \tag{10}$$

where

$$\begin{aligned} &e^{2i\alpha}=\frac{\zeta^2\omega'(\zeta)}{\rho^2\overline{\omega'(\zeta)}}\ ,\quad \Phi=\frac{\varphi'(\zeta)}{\omega'(\zeta)}\\ &\Psi(\zeta)=\frac{\psi'(\zeta)}{\omega'(\zeta)}\ ,\quad \Phi'=\varphi''(\zeta)\omega'(\zeta)\end{aligned} \tag{11}$$

By solving the system of Eqs. (9) and (10), the stress components in terms of stress functions and conformal mapping function will be as follows:

$$\sigma_\rho=\mathrm{Re}\left[\frac{2\varphi'(\zeta)}{\omega'(\zeta)}-\frac{\zeta^2}{\rho^2\overline{\omega'(\zeta)}}(\overline{\omega(\zeta)}\varphi''(\zeta)\omega'(\zeta)+\psi'(\zeta))\right] \tag{12}$$

$$\sigma_\theta=\mathrm{Re}\left[\frac{2\varphi'(\zeta)}{\omega'(\zeta)}+\frac{\zeta^2}{\rho^2\overline{\omega'(\zeta)}}(\overline{\omega(\zeta)}\varphi''(\zeta)\omega'(\zeta)+\psi'(\zeta))\right] \tag{13}$$

$$\tau_{\rho\theta}=\mathrm{Im}\left[\frac{\zeta^2}{\rho^2\overline{\omega'(\zeta)}}(\overline{\omega(\zeta)}\varphi''(\zeta)\omega'(\zeta)+\psi'(\zeta))\right] \tag{14}$$

Therefore, solution of plane stress problem is reduced to determination of two holomorphic analytical functions $\varphi(\zeta)$ and $\psi(\zeta)$ which satisfy the boundary conditions of the problem. Pan [16] used the conformal mapping to solve the problem of stress distribution around quasi-square holes in finite plate subjected to in-plane loadings. He introduced $\varphi(\zeta)$ and $\psi(\zeta)$ in ζ as Eqs. (15) and (16):

$$\varphi(\zeta)=\sum_{n=1}^{M}A_n\zeta^{-n}+\sum_{n=0}^{M}B_n\zeta^n \tag{15}$$

$$\psi(\zeta)=\sum_{n=1}^{M}\frac{C_n\zeta^{-n}}{\omega'(\zeta)}+\sum_{n=0}^{M}D_n\zeta^n \tag{16}$$

where M is the number of terms related to different parts of Laurent series terms. Where A_n, B_n, C_n and D_n are complex numbers which are considered as below:

$$\begin{aligned} &A_n=a_{n1}+ia_{n2}\ ,\quad B_n=b_{n1}+ib_{n2}\\ &C_n=c_{n1}+ic_{n2}\ ,\quad D_n=d_{n1}+id_{n2}\end{aligned} \tag{17}$$

$a_{n1},a_{n2},b_{n1},b_{n2},c_{n1},c_{n2},d_{n1}$ and d_{n2} are unknown real constants. According to described relations, to investigate the stress distribution around hole, the unknown coefficients A_n , B_n , C_n and D_n in Eqs. (12) to (14) need to be calculated. For this purpose, the least squares boundary method is used for both internal and external boundary

conditions [16]. σ_0 is the tensile stress applied on the external boundary of the plate. In this paper, this stress is considered to be 1 *MPa* . The external boundary conditions of the finite plate with hole are as Eqs. (18) and (19):

$$\sigma_x \cos^2\gamma + \sigma_y \sin^2\gamma + 2\tau_{xy} \sin\gamma\cos\gamma = \sigma_n \tag{18}$$

$$(\sigma_y - \sigma_x)\sin\gamma\cos\gamma + \tau_{xy}(\cos^2\gamma - \sin^2\gamma) = \tau_n \tag{19}$$

In the above equation, γ is the angle between the vector perpendicular to the external boundary of the plate and the *X*-axis. σ_n and τ_n are respectively the normal stress and the shear stress on the external boundary. The effect of rotation angle of different holes is evaluated by using two Cartesian coordinate system on the center of the plate. The *x*-*y* coordinates positioned on hole and the *X*-*Y* coordinate positioned on the plate. The rotation angle of hole is the angle between these coordinates. Consequently, according to the aforementioned formulas, a linear equation system is constructed such that the unknown constants can be obtained by its solution. In substituting these constants in Eqs. (15) and (16), two stress functions of $\varphi(\zeta)$ and are calculated and finally the stress components are obtained using Eqs. (12) to (14).

4 METAHEURISTICS ALGORITHMS

Nowadays, metaheuristic algorithms have many applications in different branches of optimization. Most of these algorithms are inspired by the order and rules found in natural organisms, and some of them are derived from other branches of science. Unlike exact optimization methods, these algorithms seek to find points that are as close to the global optimum as possible, so that the decision-makers needs are met to an acceptable level. In other words, metaheuristic methods search for near-optimum solutions with an acceptable computational cost.

Table 1
Algorithm implementation details.

GA	GSA	BA
Population size = 30	Population size = 30	Population size = 30
Maximum of iteration = 120	Maximum of iteration = 120	Maximum of iteration = 120
Probability of crossover (Pc) = 0.8	Euclidian distance = $R_{ij}(t) = \left\| x_i(t), x_j(t) \right\|$	Variable wavelength = λ
Probability of mutation (Pm) = 0.03		Pulse emission = $r_i \in [0,1]$
ncrossover = 2*round(npop*Pc/2)		
nmut = npop*Pm		

Metaheuristic methods are also known as approximate methods because of the major role played by stochastic mechanisms in their structure. So far, various metaheuristic algorithms have been devised.

Examples include the genetic algorithm inspired by genetics and evolution; the gravitational search algorithm inspired by the force of gravity and gravitation in nature and the bat algorithm inspired by the life behavior of bats in nature. Such algorithms have ways to escape local optima and can be used for a wide range of problems. Table 1. indicates the influence parameters for each optimization algorithms.

4.1 Genetic Algorithm (GA)

Genetic Algorithm (GA) is a subset of evolutionary algorithms that uses Darwin's principles of natural selection to find the most optimal solution. This algorithm was developed by John Holland. A collection of all previous research on genetic algorithm was attended by Gen [32] and Sivanandam [33]. Zhao and et al. [34] studied the reinforcement design for composite laminate with large hole by a genetic algorithm method. It can be said that this algorithm uses of genetic evolution as a problem-solving model. Toledo et al. [35] applied a genetic algorithm with hierarchically structured population to solve unconstrained optimization problems. This algorithm begins with a set of solutions (represented by chromosomes) called population. Each set of solutions includes all the variables of the genes

problem [32]. This algorithm starts by generating an initial population. With the available information on current population, new population is created. For better results, new population of parents is selected to have better responses then new children are produced for the next generation from these parents. Production of these generations continues so much to close to the desired condition and the best answer to be achieved. The process of genetic algorithm begins by selecting the number of chromosomes. Then the optimization function is obtained for each of the produced chromosomes. New stages are carried out by producing the new generation. At this stage, the concepts of selection, mutation, reproduction and migration are handled. One of the most important effective factors on the choice of the number of parents for reproduction is crossover probability. The number of population that participates in crossover is given as below:

$$ncrossover = 2 * round\,(npop * P_c / 2) \tag{20}$$

In this equation, $npop$ and P_c are the number of population and the probably crossover respectively. Crossover is the process of taking two parent solutions and producing from them a child. The traditional genetic algorithm uses single point crossover, where the two mating chromosomes are cut once at corresponding points and the sections after the cuts exchanged. After crossover, the strings are subjected to mutation. Mutation prevents the algorithm to be trapped in a local minimum. If crossover is supposed to exploit the current solution to find better ones, mutation is supposed to help in the exploration of the whole search space. Then the optimum of the new chromosomes is evaluated. Now, individuals from the old population are killed and replaced by the new ones. The algorithms stopped when the population converges toward the optimal solution [33].

4.2 Gravitational Search Algorithm (GSA)

Gravitational Search Algorithm (GSA) was introduced by Rashedi et al. in [36] and is intended to solve optimization problems. The gravitational search algorithm is inspired by the law of gravity and the force of gravitation in nature. In the Newton law of gravity, each particle attracts every other particle with a gravitational force. The gravitational force between two particles is directly proportional to the product of their masses and inversely proportional to the square of the distance between them [36]:

$$F = G\frac{M_1 M_2}{R^2} \tag{21}$$

where F is the magnitude of the gravitational force, G is gravitational constant, M_1 and M_2 are the mass of the first and second particles respectively, and R is the distance between the two particles. Newton's second law says that when a force, F is applied to a particle, its acceleration, a, depends only on the force and its mass M [36]:

$$a = \frac{F}{M} \tag{22}$$

Three kinds of masses are defined in theoretical physics: active gravitational mass (M_a), passive gravitational mass (M_p) and inertial mass (M_i). M_a is a measure of the strength of the gravitational field due to a particular object. M_p is a measure of the strength of an object interaction with the gravitational field and M_i is a measure of an object resistance to changing its state of motion when a force is applied. Now, considering the above-mentioned aspects, we rewrite Newton's laws. The gravitational force, F_{ij} that acts on mass i by mass j, is proportional to the product of the active gravitational of mass j and passive gravitational of mass i, and inversely proportional to the square distance between them. a_i is proportional to F_{ij} and inversely proportional to inertia mass of i. More precisely, one can rewrite Eqs. (21) and (22) as follows [36]:

$$F_{ij} = G\frac{M_{aj} M_{pi}}{R^2} \qquad a_i = \frac{F_{ij}}{M_{ii}} \tag{23}$$

where M_{aj} and M_{pi} represent the active gravitational mass of particle *j* and passive gravitational mass of particle *i*, respectively and M_{ii} represents the inertia mass of particle *i*. In the GSA algorithm, agents are considered as objects and their performance is measured by their masses. In fact, each mass presents a solution, and the algorithm is navigated by properly adjusting the gravitational and inertia masses. By lapse of time, we expected that masses be attracted by the heaviest mass. This mass will present an optimum solution in the search space. The masses obey the law of gravity and law of motion. Therefore, consider a system with *N* agents (masses). We define the position of the i^{th} (i =1, 2,…, N) agent by Eq.(24) [36]:

$$x_i = (x_i^1 \cdots \quad x_i^d \cdots \quad x_i^n) \tag{24}$$

where x_i^d presents the position of i^{th} agent in the d^{th} dimension. At a specific time *t*, we define the force acting on mass *i* from mass *j* as Eq. (25) [37]:

$$F_{ij}^d(t) = G(t)\frac{M_{aj}(t) \times M_{pi}(t)}{R_{ij}(t) + \beta}(x_j^d(t) - x_i^d(t)) \tag{25}$$

where M_{aj} is the active gravitational mass related to agent j, M_{pi} is the passive gravitational mass related to agent i, $G(t)$ is gravitational constant at time *t*, β is a small constant, and $R_{ij}(t)$ is the Euclidean distance between two agents *i* and *j* as Eq.(26) [37]:

$$R_{ij}(t) = \left\| x_i(t), x_j(t) \right\| \tag{26}$$

To give a stochastic characteristic to GSA algorithm, Rashedi et al. [36] supposed that the total force that acts on agent i in a dimension d be a randomly weighted sum of d^{th} components of the forces exerted from other agents as Eq.(27) [36]:

$$F_i^d(t) = \sum_{j=1, j\neq i}^{N} rand_j F_{ij}^d(t) \tag{27}$$

where $rand_j$ is a random number in the interval [0, 1]. Hence, by the law of motion, the acceleration of the agent *i* at time *t*, and in direction d^{th}, $a_i^d(t)$ is given as follows [36]:

$$a_i^d(t) = \frac{F_i^d(t)}{M_{ii}(t)} \tag{28}$$

where M_{ii} is the inertial mass of i^{th} agent. Furthermore, the next velocity of an agent is considered as a fraction of its current velocity added to its acceleration. Therefore, its position and its velocity could be calculated as Eqs. (29) and (30) [37]:

$$v_i^d(t+1) = rand_i \times v_i^d(t) + a_i^d(t) \tag{29}$$

$$x_i^d(t+1) = x_i^d(t) + v_i^d(t+1) \tag{30}$$

where $rand_i$ is a uniform random variable in the interval [0, 1]. This random number used to give a randomized characteristic to the search. The gravitational constant *G* is initialized at the beginning and will be reduced with time to control the search accuracy. In other words, *G* is a function of the initial value (G_0) and time (*t*) as follows [36]:

$$G(t) = G(G_0, t) \tag{31}$$

Once the system has been created, each mass is randomly positioned at a point in the search space. Gravitational and inertia masses are simply calculated by the cost function. A heavier mass means a more efficient agent. This means that better agents have higher attractions and walk more slowly. Assuming the equality of the gravitational and inertia mass, the values of masses are calculated using the map of optimum. We update the gravitational and inertial masses by the following equations [36]:

$$\begin{aligned} M_{ai} &= M_{pi} = M_{ii} = M_i \\ m_i(t) &= \frac{opt_i(t) - worst(t)}{best(t) - worst(t)} \\ M_i(t) &= \frac{m_i(t)}{\sum_{j=1}^{N} m_j(t)} \end{aligned} \tag{32}$$

The mass of each agent is $m_i(t)$ and $opt_i(t)$ represent the optimum value of the agent i at time t, and, $worst(t)$ and $best(t)$ are defined for a minimization problem as Eq.(33) [36]:

$$\begin{aligned} best(t) &= \min_{i \in \{1,\ldots,N\}} opt_i(t) \\ worst(t) &= \max_{i \in \{1,\ldots,N\}} opt_i(t) \end{aligned} \tag{33}$$

4.3 Bat Algorithm (BA)

The Bat Algorithm (BA), inspired by the echolocation behavior of bats has been proposed by Yang [38]. There are many types of bats in the nature. They are different in terms of size and weight but they all have quite similar behaviors when navigating and hunting. Bats utilize natural sonar in order to do this. The three main characteristics of bats when finding prey have been adopted in designing the BA algorithm. Firstly, most of the species of the bat utilize the echolocation to detect their prey, but not all species of the bat do the same thing. However, the bat is a famous example of extensively using the echolocation. Hence, the first characteristic is the echolocation behavior. The second characteristic is the frequency that the bat sends a fixed frequency $f^{\min}$ with a variable wavelength λ and the loudness A_0 to search for prey. Thirdly, there are many ways to adjust the loudness. For simplicity, the loudness is assumed to be varied from a positive large A_0 to a minimum constant value, which is denoted by $A_{\min}$. All bats fly randomly in the search space producing random pulses. After each fly, the position of each bat is updated as Eq.(34) [38]:

$$\begin{aligned} f_i &= f^{\min} + \varphi\,(f^{\max} - f^{\min}) \\ V_i^{t'} &= V_i^{t'-1} + f_i\,(X_i^{t'} - X_{best}) \\ X_i^{t'} &= X_i^{t'-1} + V_i^{t'} \end{aligned} \tag{34}$$

where f_i is the frequency used by the bat seeking for its prey, the suffixes, *min* and *max*, represent the minimum and maximum value, respectively. X_i denotes the location of the i^{th} bat in the solution space, V_i represents the velocity of the bat, t' indicates the current iteration, φ is a random vector ($\varphi \in [0,1]$), which is drawn from a uniform distribution, and X_{best} indicates the global near best solution found so far over the whole population [38]. In addition, the rate of the pulse emission from the bat is also taken to be one of the roles in the process. The pulse emission rate is denoted by the symbol r_i, and $r_i \in [0, 1]$, where the suffix i indicates the i^{th} bat. In every iteration,

a random number is generated and compared with r_i . If the random number (ε) is greater than r_i , a local search strategy, namely, random walk is detonated. A new solution for the bat is generated by Eq. (35) [39]:

$$X^{t'+1} = X^{t'} + \varepsilon A^{t'} \tag{35}$$

where ε is a random number in the range of [−1,1], $A^{t'}$ represents the average loudness of all bats at the current time step and r_i indicates pulse emission rate in the range of [0,1]. After updating the positions of the bats, the loudness A_i and the pulse emission rate r_i are also updated only when the global near best solution is updated and the random generated number is smaller than A_i . The update of A_i and r_i are operated by Eq. (36) and Eq. (37) [39]:

$$A_i^{t'+1} = \alpha A_i^{t'} \tag{36}$$

$$r_i^{t'+1} = r_i^0 \left[1 - \exp(-\delta \times t')\right] \tag{37}$$

where α and δ are constant values and equal to 0.9 is used for the simplicity ($\alpha = \delta = 0.9$).

5 ALGHORITHMS CONVERGENCE

Accordingly, Fig. 3 shows convergence graph of the cost function for three optimization algorithm in *m*=0.12 and *b/a*=1.5. It is clear that in most runs of GA consecutive cost function values remain more or less unchanged after generation 95 and GSA with similar populations, consecutive cost function values remain more or less unchanged after generation 38 while in BA this occurs near generation 16. The running time achieved for these three algorithms was also compared, and after running the program multiple times, it was found that BA is able to find the global optimum sooner than the other two algorithms.

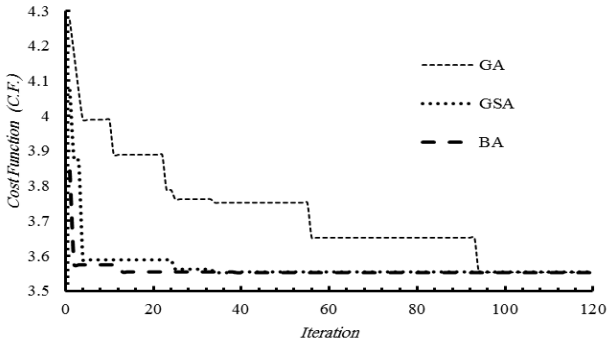

Fig.3
GA, *GSA* and *BA* convergence diagram.

6 VALIDATION OF THE RESULTS

To check the accuracy of the result, the existing cases in literatures are modeled. As an example, Fig. 4 presents a comparison between the analytical solution and finite element method for a finite perforated plate with square hole (*m=0.12*). The hole geometry was modeled in accordance with optimum parameters obtained from program execution in ABAQUS software. Comparison of the obtained values of the cost function from analytical solution method in this case and numerical solution in one of the optimized cases of ($m = 0.12 \quad b/a = 1.75 \quad L/a = 0.4$) for a finite perforated plate subjected to uniaxial load is shown in Fig. 4. Angle of θ , specifies angle of points on the border of the hole with respect to horizontal axis. Good agreements between the results obtained by the analytical solution with numerical solution show the accuracy and precision of the present analytical solution.

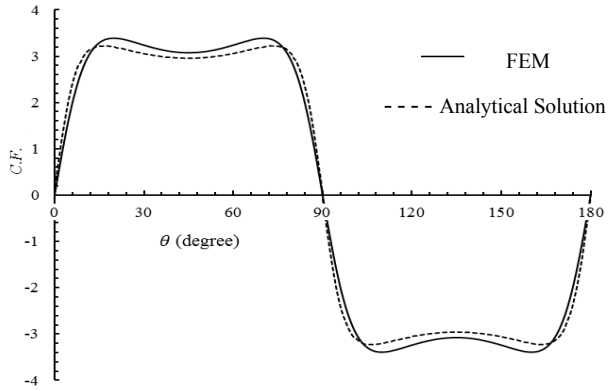

Fig.4
Compare FEM and present solution for $m=0.12 \quad b/a=1.75 \quad L/a=0.4$.

7 RESULTS

In this section tries to investigate the effected of plate dimension ratios (*b/a*) on stress analysis of a finite perforated plate with central quasi-square hole with $L/a=0.4$ by using GA as evolutionary algorithm category, GSA as physics-based algorithm category and BA as swarm intelligence algorithm category. It is worth discussing here that the effective parameters on stress distribution around holes include plate dimension ratio, curvature radius of the corner of the hole and rotation angle of the hole subjected to uniaxial loading. Mechanical properties used in this study are presented in Table 2.

Table 2
Material properties.

Materials	*E*(*MPa*)	υ
Steel	207	0.3

when the geometry of hole is considered as design variable, by choosing the appropriate value of hole orientation, the value of stress concentration factor can be minimized. For this purpose, using genetic, gravitational search and bat algorithms in different values of (*b/a*), optimal values of hole orientation in different *m* values are investigated for a finite perforated plate with central quasi-square hole in the ratio of hole size to plate size (*L/a*) equal to 0.4. Results obtained for different *m* values from the three optimization algorithms are shown in Tables 3 to 8. According to the results of these Tables, it is observed that the optimal values of stress concentration factor in all values of bluntness parameter (*m*) occur at $b/a=3$. The most important point of these results is that the lowest value of the optimized stress concentration factor occurs in the *m=0.08*. Then, it can be concluded that the value of stress concentration factor less than circular hole (*m*=0) can be achieved by selecting the appropriate values for the effective parameters such as hole orientation angle. Furthermore, using the results of Tables 3 to 8, the optimal solution obtained from the three algorithms can be compared with each other. It can be concluded that BA as swarm intelligence category offers outperforms genetic and gravitational search algorithms in optimizing the value of stress concentration factor, frequently. According to the results, the least value of the optimized stress concentration factor equal to 3.0784 obtained from bat algorithm in $L/a=0.4, \quad b/a=3,, \quad m=0.08$.

Table 3
Optimum values corresponding cost function for *m*=0.

b/a	β	*GA*	*GSA*	*BA*
0.75	0	7.5373	7.5143	6.9103
1	36.1284	5.8451	5.814	5.7719
1.25	54.7231	4.7719	4.7789	4.6632
1.5	33.4165	4.333	4.3309	4.3281
1.75	9.3172	4.1607	4.1614	4.0008
2	29.8453	4.1185	4.1013	3.8371
3	26.7035	4.1886	4.0485	3.7423

Table 4
Optimum values of corresponding cost function for m=0.04.

b/a	β	GA	GSA	BA
0.75	59.6921	6.4564	6.4564	6.4551
1	53.4088	4.8551	4.8604	4.8195
1.25	28.2747	4.1233	4.0027	4.0027
1.5	40.8424	3.8101	3.6471	3.7533
1.75	53.4041	3.5164	3.5158	3.4719
2	28.1756	3.4711	3.4701	3.4432
3	47.1216	3.4210	3.4236	3.4179

Table 5
Optimum values of corresponding cost function for m=0.08.

b/a	β	GA	GSA	BA
0.75	59.6901	6.6121	6.5208	5.9423
1	9.4264	4.4471	4.4433	4.4439
1.25	53.4041	3.7177	3.6134	3.6513
1.5	28.2747	3.3592	3.271	3.2581
1.75	28.2712	3.2841	3.1818	3.1417
2	9.4251	3.2174	3.1001	3.0986
3	34.5565	3.1128	3.0928	3.0784

Table 6
Optimum values of corresponding cost function for m=0.12.

b/a	β	GA	GSA	BA
0.75	28.3119	7.4913	7.9891	6.6227
1	9.4251	6.0541	4.8557	4.7155
1.25	28.2742	4.2996	3.9287	3.9262
1.5	47.1228	3.5573	3.5545	3.6834
1.75	53.4041	3.4179	3.4211	3.4155
2	9.4264	3.362	3.362	3.2701
3	59.6904	3.3411	3.3403	3.2377

Table 7
Optimum values of corresponding cost function for m=0.16.

b/a	β	GA	GSA	BA
0.75	53.4088	10.9123	10.7954	10.7937
1	9.4251	5.8211	5.8209	5.8226
1.25	21.9906	4.6871	4.6877	4.6675
1.5	23.8116	4.2627	4.2502	4.1883
1.75	47.1228	4.1219	4.086	3.8513
2	34.5565	4.0277	4.027	3.6097
3	28.2747	3.9135	4.0062	3.5226

Table 8
Optimum values of corresponding cost function for m=0.2.

b/a	β	GA	GSA	BA
0.75	9.4211	16.0562	16.1346	15.7719
1	40.8607	7.7266	7.587	7.5881
1.25	34.5165	6.1619	6.0697	6.2046
1.5	3.142	5.5203	5.5163	5.5037
1.75	34.5559	5.3277	5.3144	5.3101
2	53.4054	5.2444	5.2454	5.2384
3	47.1246	5.2276	5.2227	5.2218

Figs. 5 to 7 show the values of the cost function (optimum stress values) in terms of plate dimension ratios in various curvatures by genetic, gravitational search and bat algorithms, respectively. According to Figs. 5 to 7, the highest values of optimum stress occur in *m=0.2* and the lowest values of optimum stress occur in *m=0.08*. It means that quasi-square hole in special bluntness, optimum stress will be obtained. Then, the value of stress concentration factor less than circular hole (*m*=0) can be achieved by selecting appropriate values for the effective parameters such as rotation angle.

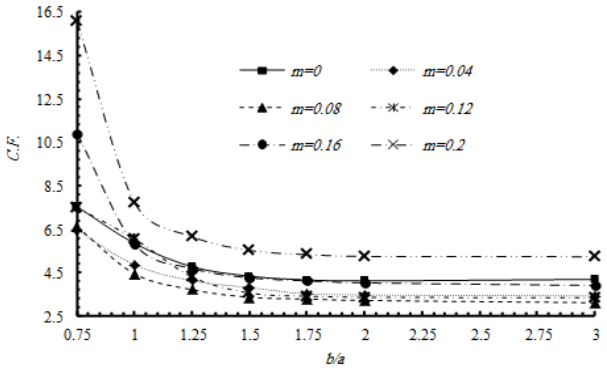

Fig.5
The effective plate dimension ratio in various curvature radius of the corner by genetic algorithm (GA).

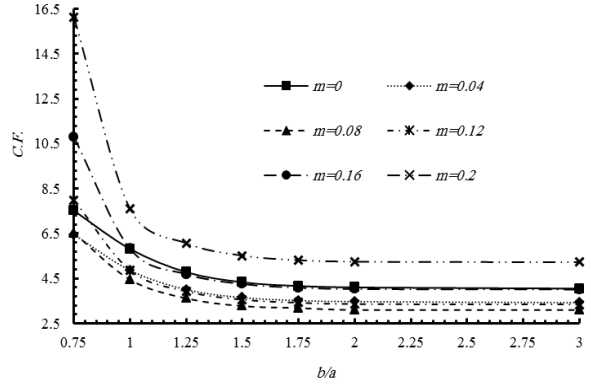

Fig.6
The effective plate dimension ratio in various curvature radius of the corner by gravitational search algorithm(GSA).

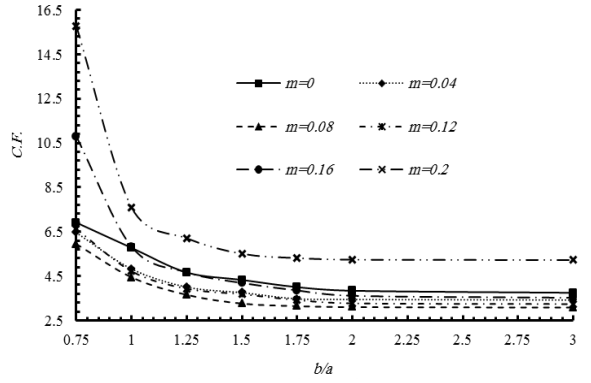

Fig.7
The effective plate dimension ratio in various curvature radius of the corner by bat algorithm (BA).

Finally, Table 9. shows overall optimum results for the perforated material. The optimum values of curvature radius of the corner of the hole and the hole orientation obtained by GA, GSA and BA. According to the Table 9, for perforated material, by increasing plate dimension ratio, the value of the cost function decreases. Also, among the three groups of metaheuristic algorithms expressed in this paper, the bat algorithm as SI algorithm category leads to the most optimal result than the other two algorithms.

Table 9
Overall optimum results by metaheuristic optimization algorithm.

b/a	β	m	*GA*	*GSA*	*BA*
0.75	58.4097	0.05836149	6.3498	6.3342	6.313
1	75.3532	0.07232119	4.5412	4.4909	4.4722
1.25	34.5567	0.08054442	3.6222	3.6218	3.6205
1.5	29.6753	0.07853241	3.2987	3.2773	3.2773
1.75	53.8951	0.07932772	3.1816	3.1417	3.1413
2	21.9892	0.08054387	3.1291	3.0991	3.0985
3	38.6405	0.07975969	3.0913	3.0848	3.078

8 CONCLUSIONS

This paper applied three metaheuristic optimization algorithms categories. Using GA, GSA and BA, The optimal values of parameters affecting the stress distribution around quasi- square hole located in a finite perforated plate subjected to uniaxial loading were discussed. Moreover, the results of these algorithms were compared with each other. The results obtained in this paper showed that BA is other forms of metaheuristic algorithms based on swarm intelligence which has the advantages such as high exploration and exploitation in comparison with other used algorithms. Besides, avoiding from the local optimum in many cases, indicated the superiority of this algorithm to other cases. The design variables are the curvature of hole corners, rotation angle of hole, plate dimension ratio and the ratio of cut-out size to plate size. The considered cost function was obtained based on Muskhelishvili's complex variable and conformal mapping with plane stress assumption. The stress functions in ζ-plane were determined by superposition of the stress function in infinite plate containing square hole with stress function in finite plate without hole. Using least square boundary collocation method and applying appropriate boundary conditions, unknown coefficients of stress function were obtained. The results also showed that the hole bluntness is not the only parameter affecting the reduction of stress concentration, but also the hole orientation play a role in the reduction of stress that with choosing the optimum values of these parameters in a specific curvature, stress concentration can be reduced significantly.

REFERENCES

[1] Muskhelishvili N., 1954, *Some Basic Problems of the Mathematical Theory of Elasticity*, Dordrecht, Springer, Netherlands.
[2] Savin G.N., 1961, *Stress Concentration Around Holes*, Pregamon Press.
[3] Lekhnitskiy S.G., 1969, *Anperforated Plates*, New York, Gordon-Breach Science.
[4] Theocaris P.S, Petrou L., 1986, Stress distributions and intensities at corners of equilateral triangular holes, *International Journal of Fracture* **31**(1): 271-289.
[5] Daoust J., Hoa S.V., 1991, An analytical solution for anperforated plates containing triangular holes, *Composite Structures* **19**(1): 107-130.
[6] Abuelfoutouh N.M., 1993, Preliminary design of unstiffened composite shells, *Symposium of 7th Technical Conference of ASC*.
[7] Rezaeepazhand J., Jafari M., 2005, Stress analysis of perforated composite plates, *Composite Structures* **71**(1): 463-468.
[8] Rezaeepazhand J., Jafari M., 2010, Stress concentration in metallic plates with special shaped cutout, *International Journal of Mechanical Sciences* **52**(1): 96-102.
[9] Odishelidze N., Criado F., 2016, Stress concentration in an elastic square plate with a full-strength hole, *Mathematics and Mechanics of Solids* **21**: 552-561.
[10] Sharma D.S., 2011, Stress concentration around circular / elliptical / triangular cutouts in infinite composite plate, *Proceedings of the World Congress on Engineering*.
[11] Kradinov V., Madenci E., Ambur D.R., 2007, Application of genetic algorithm for optimum design of bolted composite lap joints, *Composite Structures* **77**: 148-159.
[12] Yun K., 2009, Optimal bound on high stresses occurring between stiff fibers with arbitrary shaped cross-sections, *Journal of Mathematical Analysis and Applications* **350**: 306-312.
[13] Fuschi P., Pisano A.A., Domenico D. De., 2015, Plane stress problems in nonlocal elasticity : finite element solutions with a strain-difference-based formulation, *Journal of Mathematical Analysis and Applications* **1**: 1-23.

[14] Bazehhour B.G., Rezaeepazhand J., 2014, Torsion of tubes with quasi-polygonal holes using complex variable method, *Mathematics and Mechanics of Solids* **19**: 260-276.
[15] Ghugal Y.M., Sayyad A.S., 2010, A static flexure of thick perforated plates using trigonometric shear deformation theory, *Journal of Solid Mechanics* **2**: 79-90.
[16] Pan Z., Cheng Y., Liu J., 2013, Stress analysis of a finite plate with a rectangular hole subjected to uniaxial tension using modified stress functions, *International Journal of Mechanical Sciences* **75**: 265-277.
[17] Jafari M., Ardalani E., 2016, Stress concentration in finite metallic plates with regular holes, *International Journal of Mechanical Sciences* **106**: 220-230.
[18] Liu Y., Jin F., Li Q., 2006, A strength-based multiple cutout optimization in composite plates using fixed grid finite element method, *Composite Structures* **73**: 403-412.
[19] Sivakumara K., Iyengar N.G.R., Deb K., 1998, Optimum design of laminated composite plates with cutouts using a genetic algorithm, *Composite Structures* **42**: 265-279.
[20] Almeida F.S., Awruch A.M., 2009, Design optimization of composite laminated structures using genetic algorithms and finite element analysis, *Composite Structures* **88**: 443-454.
[21] Jianqiao C., Yuanfu T., Rui G., Qunli A., 2013, Reliability design optimization of composite structures based on PSO together with FEA, *Chinese Journal of Aeronautics* **26**: 343-349.
[22] Holdorf R., Lemosse D., Eduardo J., Cursi S.D., Rojas J., 2011, An approach for the reliability based design optimization, *Optimization and Engineering* **43**: 1079-1094.
[23] Vosoughi A.R., Gerist S., 2014, New hybrid FE-PSO-CGAs sensitivity base technique for damage detection of laminated composite beams, *Composite Structures* **118**: 68-73.
[24] Sharma D.S., Patel N.P., Trivedi R.R., 2014, Optimum design of laminates containing an elliptical hole, *International Journal of Mechanical Sciences* **85**: 76-87.
[25] Jafari M., Rohani A., 2016, Optimization of perforated composite plates under tensile stress using genetic algorithm, *Journal of Composite Materials* **50**: 2773-2781.
[26] Suresh S., Sujit P.B., Rao A.K., 2007, Particle swarm optimization approach for multi-objective composite box-beam design, *Composite Structures* **81**: 598-605.
[27] Vigdergauz S., 2012, Stress-smoothing holes in an elastic plate: From the square lattice to the checkerboard, *Mathematics and Mechanics of Solids* **17**: 289-299.
[28] Zhu X., He R., Lu X., Ling X., Zhu L., Liu B., 2015, A optimization technique for the composite strut using genetic algorithms, *Materials and Design* **65**: 482-488.
[29] Izquierdo J., Campbell E., Montalvo I., Pérez-García R., 2016, Injecting problem-dependent knowledge to improve evolutionary optimization search ability, *Journal of Computational and Applied Mathematics* **291**: 281-292.
[30] Yang W., Yue Z., Li L., Wang P., 2015, Aircraft wing structural design optimization based on automated finite element modelling and ground structure approach, *Optimization and Engineering* **273**: 1-21.
[31] Rezaeipouralmasi A., Fariba F., Rasoli S., 2015, Modifying stress-strain curves using optimization and finite elements simulation methods, *Journal of Solid Mechanics* **7**: 71-82.
[32] Gen M., Cheng R., 2000, *Genetic Algorithms and Engineering Optimization*, New York, John Wiley & Sons.
[33] Sivanandam S.N., Deepa S.N., 2008, *Genetic Algorithm Optimization Problems, In Introduction to Genetic Algorithms*, Springer Berlin Heidelberg, New York.
[34] Sun Z.L., Zhao M.Y., Luo L.L., 2013, Reinforcement design for composite laminate with large Cutout by a genetic algorithm method, *Advanced Materials Research* **631**: 754-758.
[35] Toledo C.F.M., Oliveira L., França P.M., 2014, Global optimization using a genetic algorithm with hierarchically structured population, *Journal of Computational and Applied Mathematics* **261**: 341-351.
[36] Rashedi E., Nezamabadipour H., Saryazdi S., 2009, GSA: A gravitational search algorithm, *Information Science* **179**: 2232-2248.
[37] Sabri N.M., Puteh M., Mahmood M.R., 2013, A review of gravitational search algorithm, *International Journal of Advances in Soft Computing and its Applications* **5**: 1-39.
[38] Yang X.S., 2010, A new metaheuristic bat-inspired algorithm, *Inspired Cooperative Strategies for Optimization* **284**: 65-74.
[39] Yang X., Gandomi A.H., 2012, Bat algorithm: a novel approach for global engineering optimization, *Engineering Computations* **29**: 464-483.